Yagasaki, K., & Wagenknecht, T. (2005). Detection of symmetric homoclinic orbits to saddle-centres in reversible systems.

Detection of symmetric homoclinic orbits to saddle-centres in reversible systems

Kazuyuki Yagasaki

Department of Mechanical and Systems Engineering, Gifu University, Gifu 501-1193, Japan
Email: yagasaki@cc.gifu-u.ac.jp

Thomas Wagenknecht

Department of Engineering Mathematics, University of Bristol, Bristol BS8 1TR, UK
Email: t.wagenknecht@bristol.ac.uk

Abstract

We present a perturbation technique for the detection of symmetric homoclinic orbits to saddle-centre equilibria in reversible systems of ordinary differential equations. We assume that the unperturbed system has primary, symmetric homoclinic orbits, which may be either isolated or appear in a family, and use an idea similar to that of Melnikov's method to detect homoclinic orbits in their neighbourhood. This technique also allows us to identify bifurcations of unperturbed or perturbed, symmetric homoclinic orbits. Our technique is of importance in applications such as nonlinear optics and water waves since homoclinic orbits to saddle-centre equilibria describe embedded solitons (ESs) in systems of partial differential equations representing physical models, and except for special cases their existence has been previously studied only numerically using shooting methods and continuation techniques. We apply the general theory to two examples, a four-dimensional system describing ESs in nonlinear optical media and a six-dimensional system which can possess a one-parameter family of symmetric homoclinic orbits in the unperturbed case. For these examples, the analysis is compared with numerical computations and an excellent agreement between both results is found.

Key words: homoclinic orbit, perturbation technique, reversible system, saddle-centre, embedded soliton

PACS: 02.30.Hq, 04.25.-g, 42.50.Rh

1 Introduction

A new class of solitary waves (or 'solitons') has been found recently in a number of examples from nonlinear optics and water wave theory (see [4] and references therein). These waves are *embedded* in the continuous spectrum, that is, their wave speed or internal frequency is in resonance with small linear waves. Consequently, they have been called *embedded solitons* (ESs).

ESs are typically presented by homoclinic solutions to saddle-centre equilibria in the associated ordinary differential equation (ODE) that describes travelling waves in the original partial differential equation (PDE). This means that ESs correspond to solutions of the travelling wave ODE that are bi-asymptotic to a non-hyperbolic equilibrium, whose spectrum is the union of a pair of imaginary eigenvalues and hyperbolic eigenvalues.

In general, the existence of such solutions would be highly degenerate. Many important examples, however, lead to a *reversible* travelling wave ODE, i.e., an ODE that is invariant under time-reversal up to some linear involution R. In this case, (symmetric) homoclinic orbits to saddle-centre equilibria (or ESs) are of codimension one. Indeed, for simplicity considering the four-dimensional case, a homoclinic orbit exists if the one-dimensional stable manifold of the equilibrium intersects the two-dimensional fixed space of the involution R. Such an intersection can be generated under variation of one parameter. Choosing this parameter to be the wave speed, one can even argue that ESs in the original PDE exist robustly and only vary their wave speed when perturbed. Observe that the corresponding homoclinic solution itself is invariant under time-reversal, and therefore it is called *symmetric* [21].

In this paper we develop a perturbation technique for the detection of symmetric homoclinic orbits to saddle-centre equilibria in reversible systems of ODEs. We find such solutions in perturbations of reversible systems possessing known, primary symmetric homoclinic orbits, which may be either isolated or appear in a family. The method derives an approximation of the perturbed stable manifold, based on an idea similar to that of the Melnikov method, a well-known tool for the detection of homoclinic orbits to hyperbolic equilibria or periodic orbits (see e.g. [11, 23]). Using the technique, we can detect bifurcations of the primary or other symmetric homoclinic orbits.

To the best of our knowledge, this is the first time that an analytical technique for the detection of ESs is presented. In fact, such solutions are usually found via numerical shooting methods, which, in particular in the four-dimensional case, are very successful and straightforward to implement. In a number of examples, however, an ES is known explicitly for certain parameter values, for example because the system can be reduced to a lower-dimensional subspace.

The technique presented here can be used to detect ESs bifurcating from the primary orbit and can thus support the numerical (bifurcation) analysis, which usually relies on continuation techniques, as implemented in the software package `AUTO/HomCont` [6].

We discuss two examples to demonstrate the developed technique. The first example is a four-dimensional system of ODEs and describes embedded vortex solitons in optical media with competing quadratic and self-defocussing cubic nonlinearities. Here we predict bifurcations of ESs from an analytically known ES solution. The second example is a six-dimensional system of ODEs and illustrates the power of the method, which also allows us to analyse the persistence of symmetric homoclinic orbits appearing in a family. For this academic example, which possesses a one-parameter family of symmetric homoclinic orbits in the unperturbed system, we compute bifurcations of the primary and non-primary symmetric homoclinic orbits. In the two examples, the analytical results are compared to numerical results obtained with `AUTO/HomCont` and an excellent agreement between both results is found.

The outline of the paper is as follows: In Section 2 below we introduce the problem under consideration in detail. Afterwards, in Section 3 the theory for the detection of symmetric homoclinic orbits is presented. The general result is applied to the four-dimensional example in Section 4 and to the six-dimensional example in Section 5. Finally, we give a summary and draw conclusions in Section 6.

2 The general setup

We consider systems of the form

$$\dot{x} = f(x) + \varepsilon g(x;\mu), \quad x \in \mathbb{R}^{2n+2}, \quad \mu \in \mathbb{R}, \tag{2.1}$$

where $0 < \varepsilon \ll 1$, $f : \mathbb{R}^{2n+2} \to \mathbb{R}^{2n+2}$ and $g : \mathbb{R}^{2n+2} \times \mathbb{R} \to \mathbb{R}^{2n+2}$ are C^r ($r \geq 2$), and μ is a parameter. Assumptions (A1)–(A4) below describe the problem we are interested in.

(A1) The system (2.1) is *reversible*, i.e., there exists a (linear) involution $R : \mathbb{R}^{2n+2} \to \mathbb{R}^{2n+2}$ such that

$$f(Rx) + Rf(x) = g(Rx;\mu) + Rg(x;\mu) = 0 \text{ for all } x, \mu.$$

Moreover, $\dim \mathrm{Fix}(R) = n+1$, where $\mathrm{Fix}(R) = \{x \in \mathbb{R}^{2n+2} | Rx = x\}$.

A fundamental characteristic of reversible systems is that if $x(t)$ is a solution, then so is $Rx(-t)$. We call a solution (and the corresponding orbit) *symmetric*

if $x(t) = Rx(-t)$. It is well-known that an orbit is symmetric if and only if it intersects the space $\mathrm{Fix}(R)$ (see [21]).

When $\varepsilon = 0$, Eq. (2.1) becomes

$$\dot{x} = f(x), \tag{2.2}$$

which we refer to as the *unperturbed system*. The remaining assumptions concern (2.2).

(A2) The origin O is an equilibrium of *saddle-centre type* in (2.2). More precisely, the Jacobian matrix $A := Df(0)$ has one pair of purely imaginary eigenvalues $\pm i\omega$ and $2n$ hyperbolic eigenvalues

$$\sigma(A) = \pm i\omega \cup \{-\lambda_1, -\lambda_2, \ldots, -\lambda_n\} \cup \{\lambda_1, \lambda_2, \ldots, \lambda_n\},$$

where λ_i, $\omega > 0$.

Note that O is a symmetric equilibrium, and therefore the eigenvalues of the Jacobian matrix are symmetric with respect to the imaginary axis. Thus, assumption (A2) describes a scenario, which is structurally stable in the class of reversible systems and persists for small ε. Furthermore, by (A2) the saddle-centre O has n-dimensional stable and unstable manifolds, $W^s_{\varepsilon,\mu}(O)$ and $W^u_{\varepsilon,\mu}(O)$, and a two-dimensional centre manifold $W^c_{\varepsilon,\mu}(O)$ for ε close to 0. The reversibility of the system implies that $W^u_{\varepsilon,\mu}(O) = RW^s_{\varepsilon,\mu}(O)$ and $W^c_{\varepsilon,\mu}(O) = RW^c_{\varepsilon,\mu}(O)$.

We finally assume the existence of homoclinic solutions of (2.2) as follows.

(A3) There exists an l-parameter family of symmetric homoclinic orbits $\Gamma(\theta) = \{x^h(t;\theta),\ t \in \mathbb{R}\}$, $\theta \in \Theta$, in (2.2), where $x^h(t;\theta) \to O$ as $t \to \pm\infty$ for each $\theta \in \Theta$. Here Θ is an open subset of $\mathbb{R}^l$, with $0 \le l < n$. We further assume that

(i) $x^h(t;\theta)$ is C^r with respect to θ,
(ii) the $l+1$ vectors in $\mathbb{R}^{2n+2}$ given by

$$\frac{\partial x^h}{\partial t}(t;\theta) = f(x^h(t;\theta)), \quad \frac{\partial x^h}{\partial \theta}(t;\theta) \tag{2.3}$$

are linearly independent for $t \in \mathbb{R}$ and $\theta \in \Theta$.

The case of $l = 0$, in which the unperturbed system possesses a single or isolated homoclinic orbit $\Gamma = \{x^h(t), t \in \mathbb{R}\}$ to the saddle-centre O, is permitted.

(A4) Let $W^s_0(O)$ and $W^u_0(O)$ denote the stable and unstable manifolds of O for $\varepsilon = 0$. For $\theta \in \Theta$, the intersection between $W^s_0(O)$ and $W^u_0(O)$ along

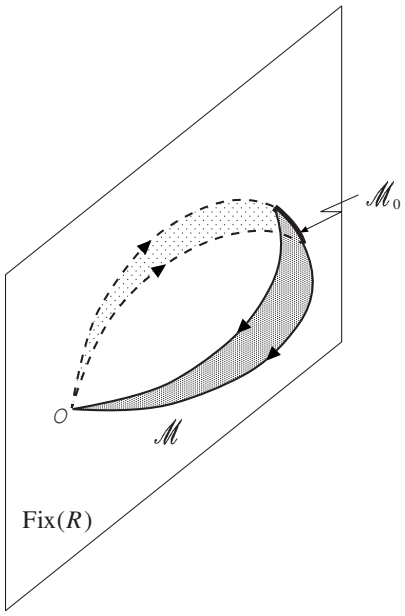

Fig. 1. The unperturbed phase space: A symmetric homoclinic manifold (or a single homoclinic orbit) $\mathscr{M}$ to O exists.

$x^h(t;\theta)$ is of dimension $l+1$, i.e.,

$$\dim\left(T_{x^h(0;\theta)}W_0^s(O)\cap T_{x^h(0;\theta)}W_0^u(O)\right)=l+1.$$

The $l+1$ vectors given by (2.3) form a basis of the $(l+1)$-dimensional space $T_{x^h(t;\theta)}W_0^s(O)\cap T_{x^h(t;\theta)}W_0^u(O)$.

Assumption (A4) is a non-degeneracy condition which requires the intersection between $W_0^s(O)$ and $W_0^u(O)$ along the family of homoclinic orbits to be as low-dimensional as possible. Note that the homoclinic solutions can be parameterised such that $x^h(0;\theta)\in$ Fix(R). It follows from (A3) and (A4) that $\dim\left(\mathrm{Fix}(R)\cap W_0^s(O)\right)=\dim\left(\mathrm{Fix}(R)\cap W_0^u(O)\right)=l$. Let

$$\mathscr{M}=\{x^h(t;\theta)\,|\,t\in\mathbb{R},\theta\in\Theta\}\cup O$$

and

$$\mathscr{M}_0=\mathscr{M}\cap\mathrm{Fix}(R)=\{x^h(0;\theta)\,|\,\theta\in\Theta\}.$$

We call the $(l+1)$-dimensional manifold $\mathscr{M}$ a *homoclinic manifold*. See Fig. 1 for the phase space of the unperturbed system (2.2).

3 Detection of homoclinic orbits

In this section we present a technique for the detection of homoclinic orbits when $\varepsilon\neq 0$. Such orbits will be found by looking for intersections of the stable

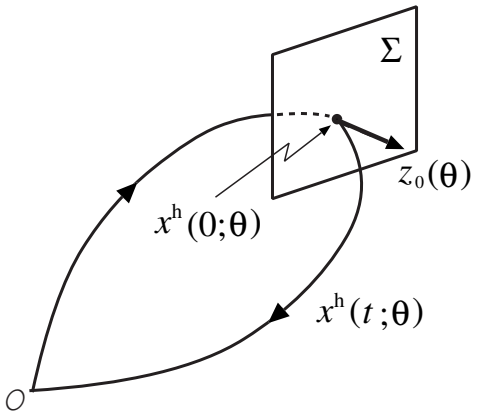

Fig. 2. Definition of Σ.

manifold $W^s_{\varepsilon,\mu}(O)$ with $\mathrm{Fix}(R)$. Since $\dim W^s_{\varepsilon,\mu}(O) = n$ and $\dim \mathrm{Fix}(R) = n+1$ one parameter is needed to create such an intersection in $\mathbb{R}^{2n+2}$. That is, the existence of symmetric homoclinic orbits to saddle-centre equilibria in reversible systems is of codimension one. In particular, we can expect such orbits to exist along curves in the (ε, μ)-parameter space. Similarly, the existence of a homoclinic manifold of dimension $l+1$ is of codimension $l+1$. Regarding $\theta \in \Theta \subset \mathbb{R}^l$ as parameters, the same considerations show that we can expect codimension-one bifurcations of ESs for discrete values of θ. Our method will compute parameter values μ at which curves of homoclinic orbits intersect the primary existence curve of homoclinic orbits, $\varepsilon = 0$, in the (ε, μ)-parameter space.

We first introduce a cross section Σ to the homoclinic manifold. Note, that by assumption (A1) there exists a splitting $\mathbb{R}^{2n+2} = \mathrm{Fix}(R) \oplus \mathrm{Fix}(-R)$, and we can choose a scalar product "$\cdot$" such that

$$\mathrm{Fix}(-R) = \mathrm{Fix}(R)^{\perp}. \tag{3.1}$$

Let $z_0(\theta) = \dot{x}^h(0;\theta)/|\dot{x}^h(0;\theta)|$ and set $Z(\theta) = \mathrm{span}\{z_0(\theta)\}$. Define a $(2n-l+1)$-dimensional space $\bar{Z}(\theta)$ by

$$\mathbb{R}^{2n+2} = Z(\theta) \oplus T_{x^h(0;\theta)}\mathscr{M}_0 \oplus \bar{Z}(\theta),$$

where we choose the decomposition to be orthogonal. Then a $(2n+1)$-dimensional cross-section Σ to $\cup_{\theta\in\Theta}\Gamma(\theta)$ is given by

$$\Sigma = \{x^h(0;\theta) + z \,|\, z \in \bar{Z}(\theta), \theta \in \Theta\}.$$

See Fig. 2.

Lemma 3.1 ([21]) *We have* $\Sigma \supset \mathrm{Fix}(R)$.

PROOF. First recall that $x^h(0;\theta) \in \mathrm{Fix}(R)$. Since

$$R\dot{x}^h(0;\theta) = R(f(x^h(0;\theta))) = -f(R(x^h(0;\theta))) = -f(x^h(0;\theta)) = -\dot{x}^h(0;\theta),$$

we see that $\dot{x}^h(0;\theta) \in \mathrm{Fix}(-R)$, i.e., $Z(\theta) \subset \mathrm{Fix}(R)^\perp$. From this the assertion of the lemma follows immediately.

For $\varepsilon > 0$ sufficiently small, let $x^s_\varepsilon(t;\mu,\theta)$ and $x^u_\varepsilon(t;\mu,\theta)$ be, respectively, orbits on the stable and unstable manifolds, $W^s_{\varepsilon,\mu}(O)$ and $W^u_{\varepsilon,\mu}(O)$, such that $x^{s,u}_\varepsilon(0;\mu,\theta) \in \Sigma$ in an $\mathscr{O}(\varepsilon)$-neighbourhood of $x^h(0;\theta)$. Using the Gronwall lemma [5], we can obtain the following estimates for $x^{s,u}_\varepsilon(t;\mu,\theta)$ (cf. [11, 23]).

Lemma 3.2 *For $\varepsilon > 0$ sufficiently small, we can express the orbits $x^{s,u}_\varepsilon(t;\mu)$ as follows:*

$$x^s_\varepsilon(t;\mu,\theta) = x^h(t;\theta) + \varepsilon\xi^s(t;\mu,\theta) + \mathscr{O}(\varepsilon^2)$$

for $t \in [0,\infty)$;

$$x^u_\varepsilon(t;\mu,\theta) = x^h(t;\theta) + \varepsilon\xi^u(t;\mu,\theta) + \mathscr{O}(\varepsilon^2)$$

for $t \in (-\infty, 0]$. Here $\xi^{s,u}(t;\mu,\theta)$ are solutions of the variational equation (VE)

$$\dot{\xi} = Df(x^h(t;\theta))\xi + g(x^h(t;\theta);\mu) \tag{3.2}$$

with $\xi^{s,u}(0;\mu,\theta) \in \bar{Z}(\theta)$.

Let $\Psi(t;\theta)$ be the fundamental matrix for the variational equation of the unperturbed system (2.2) around the homoclinic orbit $x^h(t;\theta)$ (i.e., the homogeneous part of (3.2)),

$$\dot{\xi} = Df(x^h(t;\theta))\xi, \tag{3.3}$$

such that $\Psi(0;\theta) = I$, where I denotes the identity matrix. Hence, $\Psi(t;\theta)\xi_0$ is a solution of (3.3) with $\xi(0) = \xi_0$. Denote $\xi^{s,u}_0(\mu,\theta) = \xi^{s,u}(0;\mu,\theta) \in \bar{Z}(\theta)$. In Lemma 3.2 we have

$$\xi^{s,u}(t;\mu,\theta) = \Psi(t;\theta)\left[\int_0^t \Psi^{-1}(s;\theta)g(x^h(s;\theta);\mu)ds + \xi^{s,u}_0(\mu,\theta)\right]. \tag{3.4}$$

Let $\Psi_0(t)$ be the fundamental matrix of the linearised system around the origin O for the unperturbed system (2.2),

$$\dot{\xi} = Df(0)\xi. \tag{3.5}$$

Noting that $\lim_{t\to\infty} x^h(t;\theta) = 0$ and using a fundamental result on linear differential equations [5], we can show that for each $\theta \in \Theta$ there exists a nonsingular $(2n+2)\times(2n+2)$ matrix $B(\theta)$ such that

$$\lim_{t\to\infty} \Psi_0(-t)\Psi(t;\theta) = B(\theta), \tag{3.6}$$

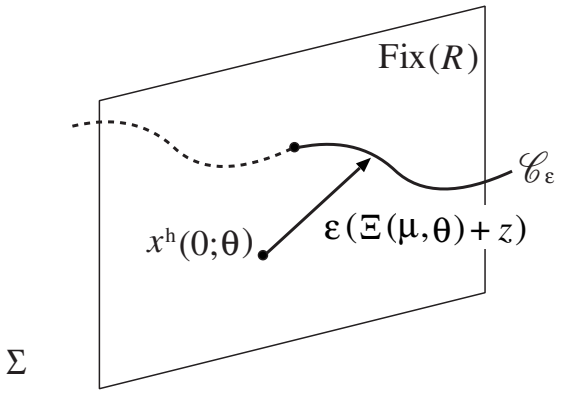

Fig. 3. Intersection of $\mathscr{C}_\varepsilon$ with Fix(R) in Σ.

(cf. Lemma 3.1 of [26]). From this we conclude that $\lim_{t\to\infty}\Psi(t;\theta)\xi_0 = 0$ if and only if $B(\theta)\xi_0 \in E^s$, where E^s denotes the stable eigenspace of (3.5). On the other hand, let $Z^s(\theta) = T_{x^h(0;\theta)}W_0^s(O)$ denote the tangent space of the unperturbed stable manifold of O at the point $x^h(0;\theta)$. For all points $\xi_0 \in Z^s(\theta)$ we have $\lim_{t\to\infty}\Psi(t;\theta)\xi_0 = 0$. Since both $Z^s(\theta)$ and E^s are of dimension n, we see that

$$\lim_{t\to\infty}\Psi(t;\theta)\xi_0 = 0 \Leftrightarrow \xi_0 \in Z^s(\theta).$$

Using (3.4) and the fact that $\lim_{t\to\infty}\xi^s(t;\mu,\theta) = 0$, we derive

$$\int_0^\infty \Psi^{-1}(t;\theta)g(x^h(t;\theta);\mu)dt + \xi_0^s(\mu,\theta) \in Z^s(\theta). \tag{3.7}$$

Let

$$\Xi(\mu,\theta) = \int_0^\infty \Psi^{-1}(t;\theta)g(x^h(t;\theta);\mu)dt, \tag{3.8}$$

and let us denote by P_θ^s the orthogonal projection with $\mathrm{Im}\,(P_\theta^s) = Z^s(\theta)$. Then Eq. (3.7) can be expressed as

$$P_\theta^s\left(\Xi(\mu,\theta) + \xi_0^s(\mu,\theta)\right) = \Xi(\mu,\theta) + \xi_0^s(\mu,\theta),$$

so that

$$(I - P_\theta^s)\xi_0^s(\mu,\theta) = (P_\theta^s - I)\Xi(\mu,\theta). \tag{3.9}$$

Let $\hat{\Xi}(\mu,\theta) = (P_\theta^s - I)\Xi(\mu,\theta)$. It follows from (3.9) that there is a point $z \in Z^s(\theta)$ such that

$$\xi_0^s(\mu,\theta) = \hat{\Xi}(\mu,\theta) + z \in \bar{Z}(\theta). \tag{3.10}$$

Let

$$\mathscr{C}_\varepsilon = \bigcup_{\theta\in\Theta}\{x^h(0;\theta) + \varepsilon(\hat{\Xi}(\mu,\theta) + z) \,|\, \mu \in \mathbb{R}, z \in Z^s(\theta), \hat{\Xi}(\mu,\theta) + z \in \bar{Z}(\theta)\}.$$

We have $\mathscr{C}_\varepsilon \subset \Sigma$ and $\dim \mathscr{C}_\varepsilon = n$, since $\dim (Z^s(\theta) \cap \bar{Z}(\theta)) = n - l - 1$. Thus, $\mathscr{C}_\varepsilon$ is an n-dimensional submanifold of the $(2n+1)$-dimensional manifold Σ, which includes the $(n+1)$-dimensional space $\mathrm{Fix}(R)$ by Lemma 3.1. If $\mathscr{C}_\varepsilon$ intersects $\mathrm{Fix}(R)$ transversely in Σ when $(\mu, \theta) = (\mu_0, \theta_0)$ as shown in Fig. 3, then near $\mu = \mu_0$ the stable manifold $W^s_{\varepsilon,\mu}(O)$ does so, and consequently there exists a symmetric homoclinic orbit near $\Gamma(\theta)$. Let

$$\tilde{\mathscr{C}} = \bigcup_{\theta \in \Theta} \left(\{ \hat{\Xi}(\mu, \theta) + z \,|\, \mu \in \mathbb{R}, z \in Z^s(\theta) \} \cap \bar{Z}(\theta) \right). \tag{3.11}$$

Noting that $x^h(0; \theta_0) \in \mathrm{Fix}(R)$, we prove the following result.

Theorem 3.3 *Suppose that the n-dimensional manifold $\tilde{\mathscr{C}}$ intersects $\mathrm{Fix}(R)$ transversely at $(\mu, \theta) = (\mu_0, \theta_0)$. Then for $\varepsilon > 0$ sufficiently small, there exists a symmetric homoclinic orbit to O in an $\mathscr{O}(\varepsilon)$-neighbourhood of $\Gamma(\theta)$ for some $\mu = \mu_0 + \mathscr{O}(\varepsilon)$.*

Remark 3.4 *So far we have assumed that the unperturbed system is independent of the parameter μ. However, it is obvious that the statement of Theorem 3.3 remains valid if the unperturbed system (2.2) also depends on μ. In that case we only have to include the dependence of $\Psi(t)$ and $x^h(t)$ on μ in (3.8). Then we can detect symmetric homoclinic orbits bifurcating from the primary one with $\varepsilon = 0$ when the parameter μ is varied (see Sections 4 and 5). Furthermore, if the system depends on an additional parameter, say ν, Theorem 3.3 generally detects a branch of symmetric homoclinic orbits in the (μ, ν)-parameter plane for ε small and fixed. It may also find a branching point at which two or more branches meet (see Section 5).*

In the next two sections we study two examples and demonstrate how the method developed above can be applied. The first example in Section 4 deals with a four-dimensional system, which describes standing waves in a nonlinear optical medium. Here we will study bifurcations of homoclinic orbits to a saddle-centre equilibrium from a primary solution. These homoclinic solutions describe ESs solutions in the underlying optical system. In Section 5 afterwards we study a six-dimensional system, which is specifically designed, such that the unperturbed system can contain a one-parameter family of homoclinic orbits to a saddle centre at the origin. For this system we will not only demonstrate the effectiveness of our technique in higher-dimensional systems but also discuss the persistence of symmetric homoclinic orbits in a homoclinic manifold and detect branching points of homoclinic orbits.

4 A four-dimensional example from nonlinear optics

As the first example, we consider a four-dimensional system of ODEs,

$$\begin{aligned} &\dot{x}_1 = x_2, \quad \dot{x}_2 = x_1 - (x_1^2 + 8x_3^2)x_1 - 2\varepsilon x_1 x_3, \\ &\dot{x}_3 = x_4, \quad \dot{x}_4 = -\omega^2 x_3 - \alpha(x_1^2 + 2x_3^2)x_3 - \varepsilon x_1^2, \end{aligned} \tag{4.1}$$

where α and ω are positive constants. This example comes from a model of a nonlinear optical medium with both quadratic and cubic nonlinearities [20], in which light propagation is described by a system of PDEs

$$\begin{aligned} &i\frac{\partial u}{\partial z} + \frac{\partial^2 u}{\partial t^2} + qu + u^* v + \gamma_1(|u|^2/4 + 2|v|^2)u = 0, \\ &2i\frac{\partial v}{\partial z} + \frac{\partial^2 v}{\partial t^2} + \kappa v + u^2/2 + \gamma_2(4|v|^2 + 2|u|^2)v = 0. \end{aligned} \tag{4.2}$$

Here z is the propagation distance, t is the reduced time or the transverse coordinate, u and v are the amplitudes of complex waves corresponding to the fundamental and second harmonic fields, respectively, q is a nonlinear shift of the fundamental harmonic's propagation constant, Δ is a wave-vector mismatch between the harmonics, $\gamma_{1,2}$ are cubic (Kerr) nonlinear coefficients, and $\kappa = 2(\Delta + 2q)$. One can take $\gamma_1 = \gamma_2 = 1$ in (4.2), in which case the cubic nonlinearity is self-focusing. Searching for stationary solutions of the form $u = U(t)\exp(ikz)$ and $v = V(t)\exp(2ikz)$ in (4.2), where $U(t)$, $V(t)$ and k are real, we obtain

$$\begin{aligned} &\ddot{U} - (k-q)U + UV + \gamma_1(U^2/4 + 2V^2)U = 0, \\ &\ddot{V} + (\kappa - 4k)V + U^2/2 + \gamma_2(4V^2 + 2U^2)V = 0, \end{aligned} \tag{4.3}$$

where the dot denotes differentiation with respect to t. Finally, we scale the variables as $U \mapsto \sqrt{\gamma_1/4(k-q)}\,U$, $V \mapsto \sqrt{\gamma_1/4(k-q)}\,V$ and $t \mapsto \sqrt{k-q}\,t$, introduce new coordinates $x_1 = U$, $x_2 = \dot{U}$, $x_3 = V$ and $x_4 = \dot{V}$ and set

$$\varepsilon = \frac{1}{\sqrt{\gamma_1(k-q)}}, \quad \alpha = \frac{8\gamma_2}{\gamma_1}, \quad \omega^2 = \frac{\kappa - 4k}{k-q} \tag{4.4}$$

to obtain (4.1) when $q < k < \kappa/2$ and $\gamma_1 > 0$. The smallness of the parameter ε means that $\gamma_1 \gg 1$ or $k - q \gg 1$. Homoclinic orbits to the origin O in (4.1) correspond to ESs in the nonlinear optical model (4.2).

The system (4.1) is reversible with respect to

$$R : (x_1, x_2, x_3, x_4) \mapsto (x_1, -x_2, x_3, -x_4).$$

Furthermore, the origin O is a saddle-centre with eigenvalues ± 1 and $\pm i\omega$. When $\varepsilon = 0$, the (x_1, x_2)-plane is invariant under the flow of (4.1) and the

restriction of (4.1) to this plane reads

$$\dot{x}_1 = x_2, \quad \dot{x}_2 = x_1 - x_1^3.$$

Hence, we easily see that there exists a pair of homoclinic orbits to the saddle-centre O,

$$x_\pm^h(t) = (\pm\sqrt{2}\,\mathrm{sech}\,t, \mp\sqrt{2}\,\mathrm{sech}\,t\,\tanh t, 0, 0). \tag{4.5}$$

Thus, assumptions (A1)-(A4) hold with $l = 0$. Using the notation of Section 3 we find that $z_0 = (0, \mp 1, 0, 0)$, $Z^s = \{z_1 = z_3 = z_4 = 0\}$, $\bar{Z} = \{z_2 = 0\}$ and

$$\mathrm{Fix}(R) = \{x_2 = x_4 = 0\}, \quad \mathrm{Fix}(-R) = \{x_1 = x_3 = 0\}.$$

Note that we equip $\mathbb{R}^4$ with the Euclidean scalar product, such that condition (3.1) is fulfilled.

The VE (3.2) now becomes a system of two decoupled second order equations

$$\begin{aligned} &\dot{\xi}_1 = \xi_2, \quad \dot{\xi}_2 = (1 - 6\,\mathrm{sech}^2 t)\xi_1, \\ &\dot{\xi}_3 = \xi_4, \quad \dot{\xi}_4 = -(\omega^2 + 2\alpha\,\mathrm{sech}^2 t)\xi_3 - 2\,\mathrm{sech}^2 t. \end{aligned} \tag{4.6}$$

The fundamental matrix for the third and fourth equations in the homogeneous part of (4.6),

$$\dot{\xi}_3 = \xi_4, \quad \dot{\xi}_4 = -(\omega^2 + 2\alpha\,\mathrm{sech}^2 t)\xi_3, \tag{4.7}$$

is symplectic and has a unit determinant since the linear system (4.7) is Hamiltonian [14]. Let $\Psi_{ij}(t)$ be the (i, j)-element of the fundamental matrix $\Psi(t)$ for (4.7). Taking α as the control parameter, we have

$$\hat{\Xi}_4(\alpha) = -\Xi_4(\alpha) = 2\int_0^\infty \Psi_{33}(t;\alpha)\,\mathrm{sech}^2 t\,dt, \tag{4.8}$$

where we explicitly represent the dependence of Ψ on α. We also note that $\Psi_{33}(t;\alpha)$ is the ξ_3-component of the solution to (4.7) with $\xi_3(0) = 1$ and $\xi_4(0) = 0$. Since $z_2 = 0$ for $z \in \bar{Z}$, we see that if $\hat{\Xi}_4(\alpha)$ has a simple zero at $\alpha = \alpha_0$, then the condition in Theorem 3.3 is fulfilled and hence a symmetric homoclinic orbit exists near $x_\pm^h(t)$ in (4.1) at $\alpha = \alpha_0 + \mathscr{O}(\varepsilon)$ for $\varepsilon \neq 0$ sufficiently small.

In general, a solution of (4.7) can be expressed using the Gauss hypergeometric function,

$$\begin{aligned} F(c_1, c_2, c_3; z) =& \sum_{k=0}^{\infty} \frac{c_1(c_1+1)\cdots(c_1+k-1)c_2(c_2+1)\cdots(c_2+k-1)}{k!c_3(c_3+1)\cdots(c_3+k-1)} z^k \\ =& 1 + \frac{c_1 c_2}{c_3}\frac{z}{1!} + \frac{c_1(c_1+1)c_2(c_2+1)}{c_3(c_3+1)}\frac{z^2}{2!} + \cdots, \end{aligned} \tag{4.9}$$

which is a special solution of the Gauss hypergeometric equation,

$$z(1-z)\frac{d^2y}{dz^2}+[c_3-(c_1+c_2+1)z]\frac{dy}{dz}-c_1c_2y=0, \tag{4.10}$$

see [1, 8]. Another linearly independent solution to (4.10) near $z=0$ is given by

$$y=z^{1-c_3}F(c_1-c_3+1,c_2-c_3+1,2-c_3;z) \tag{4.11}$$

if none of c_3, $c_3-c_1-c_2$ and c_1-c_2 is an integer. See Section 15 of [1] or Chapter II of [8] for necessary information on the Gauss hypergeometric function. The $(3,3)$-component of the fundamental matrix, $\Psi_{33}(t;\alpha)$, can be written as

$$\begin{aligned}\Psi_{33}(t;\alpha)=&\frac{a_I+b_I}{(a_I+b_I)c_R+(1-a_R)c_I}(F_R(t)\cos\omega t-F_I(t)\sin\omega t)\\&+\frac{1-a_R}{(a_I+b_I)c_R+(1-a_R)c_I}(F_R(t)\sin\omega t+F_I(t)\cos\omega t)\end{aligned} \tag{4.12}$$

if $(a_I+b_I)c_R+(a_r-1)c_I\neq 0$. Here $F_R(t)$ and $F_I(t)$ are real functions such that

$$F_R(t)+iF_I(t)=F(-\rho,\rho+1,1-i\omega;(1-\tanh t)/2)$$

with

$$\rho=\frac{1}{2}(\sqrt{8\alpha+1}-1), \tag{4.13}$$

and a_R, a_I, b_I, c_R and c_I are real numbers such that

$$\begin{aligned}a_R+ia_I&=\frac{\Gamma(1-i\omega)\Gamma(-i\omega)}{\Gamma(1+\rho-i\omega)\Gamma(-\rho-i\omega)},\quad b_I=\frac{\sin\pi\rho}{\sinh\pi\omega},\\c_R+ic_I&=\frac{2^{i\omega}\sqrt{\pi}\,\Gamma(1-i\omega)}{\Gamma(1/2-\rho/2-i\omega/2)\Gamma(1+\rho/2-i\omega/2)}.\end{aligned} \tag{4.14}$$

Here $\Gamma(z)$ denotes the Gamma function,

$$\Gamma(z)=\int_0^\infty t^{z-1}e^{-t}dt.$$

See Appendix A.1 for the derivation of (4.12).

If $\rho=l-1$, i.e., $\alpha=l(l-1)/2$, with $l\in\mathbb{N}$, then Eq. (4.7) is integrable in the meaning of the differential Galois theory for linear differential equations [22], so that the general solution of (4.7) can be expressed with elementary functions, when t and ξ are complex variables. See, for example, Section 5 of [27] for the proof of this fact. In Appendix A.2 we describe how to obtain an analytical expression of $\Psi_{33}(t;l(l-1)/2)$ in this case. For $\alpha\neq l(l-1)/2$, $l\in\mathbb{N}$, however, it is impossible to represent $\Psi_{33}(t;\alpha)$ with elementary functions and it is difficult to compute the integral (4.8) analytically. So we carried out the integration numerically. Figure 4 shows the results for $\omega=0.5,1,1.5$. Here the function

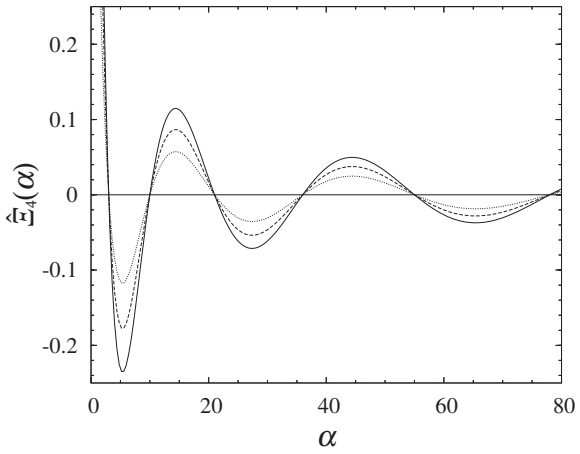

Fig. 4. Numerical computations of the integral (4.8). The solid, broken and dotted curves represent the results for $\omega = 0.5$, 1 and 1.5, respectively.

`NIntegrate` of `Mathematica` [24] was used for the numerical integration of (4.8). We see that the integral (4.8) has a simple zero near

$$\alpha = 3, 10, 21, 36, 55, 78, \ldots. \tag{4.15}$$

We conjecture that the integral (4.8) has a simple zero at $\alpha = m(2m+1)$, $m \in \mathbb{N}$.

As stated above, Eq. (4.7) is integrable in the meaning of the differential Galois theory when $\alpha = m(2m+1) = 2m(2m+1)/2$. Using the approach of Appendix A.2 to obtain an analytical expression of $\Psi_{33}(t; n(2n+1))$ and computing the integral (4.8) by the method of residue, we could prove that $\hat{\Xi}_4(n(2n+1)) = 0$ for $n \leq 6$. Thus, by Theorem 3.3, we see that the system (4.1) has a symmetric homoclinic orbit to O, which corresponds to an ES in (4.2), near $x^h_\pm(t)$ at the values of α approximately given by (4.15) for $\varepsilon > 0$ sufficiently small. Moreover, as stated in Remark 3.4, this additional orbit bifurcates from the primary one, $x^h_\pm(t)$, at the points of (4.15) on the ε-axis.

Finally in this section, we illustrate the theoretical results by computations using the numerical continuation package `AUTO/HomCont` [6]. Figure 5 shows branches of symmetric homoclinic orbits in the (α, ε)-parameter plane for the same values of ω as in Fig. 4, namely $\omega = 0.5,\ 1,\ 1.5$. As predicted by the theory additional branches bifurcate from the primary branch with $\varepsilon = 0$ at $\alpha = 3, 10, 21$. Other bifurcation values of α, i.e. $\alpha = 36, 55, 78$ have also been confirmed numerically, but are not included in the figure. In addition, panels a)–c) in the figure show plots of the bifurcating solutions for $\omega = 1$ at the parameter value $\varepsilon = 1$. We find that for increased α the amplitude of the x_3-component of these solutions decreases, while at the same time the solution develops additional oscillations around its point of symmetry. We note that these types of ESs in a nonlinear optical model very similar to (4.2) were observed numerically in [4, 29] earlier. Similar types of ESs have also been

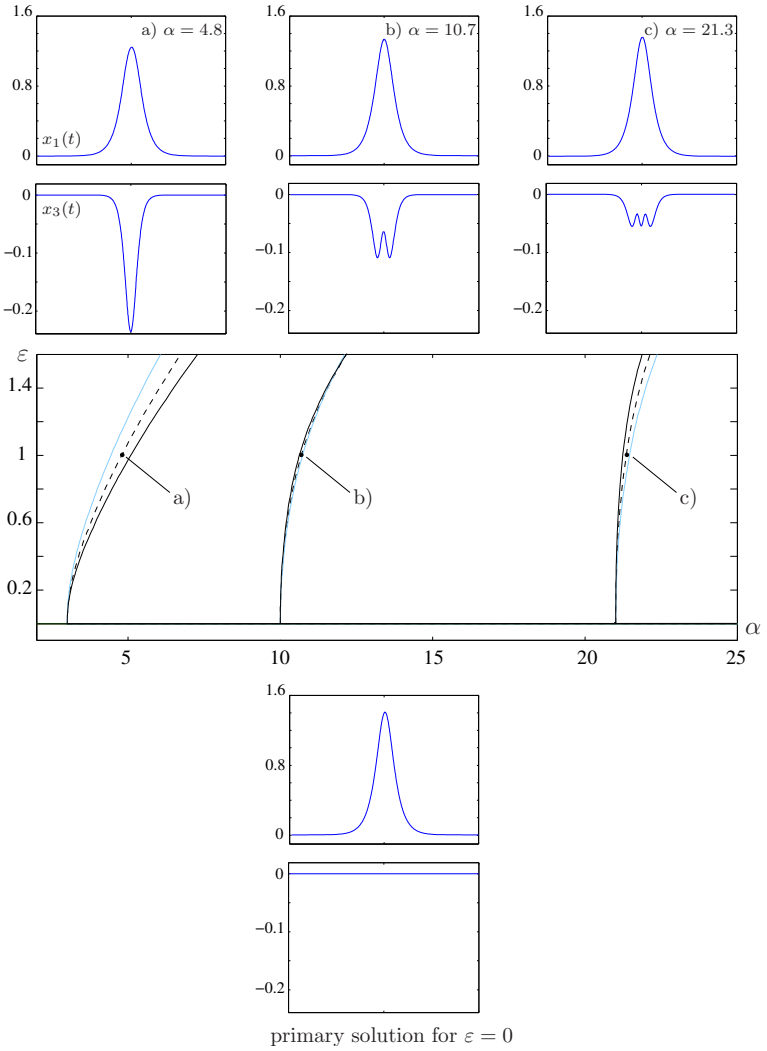

Fig. 5. Branches of symmetric homoclinic orbits of (4.1) in the (α, ε) parameter plane for several values of ω. Specifically, the bifurcation curves for $\omega = 0.5$ (grey), $\omega = 1.0$ (dashed) and $\omega = 1.5$ (black, solid) are included in the central panel. Panels a)–c) contain plots of the x_1 and x_3 component of the bifurcating solutions at $\varepsilon = 1$ for the case $\omega = 1$. The primary solution is shown underneath the bifurcation diagram.

studied in a model with quadratic nonlinearities in [3, 13].

5 A six-dimensional example

Our second application of the theory concerns a six-dimensional system of ODEs, which is specifically designed such that the unperturbed system (2.2)

possesses a two-dimensional homoclinic manifold. The equations read

$$\begin{aligned} &\dot{x}_1 = x_2, \quad \dot{x}_2 = x_1 - (x_1^2 + x_3^2 + 8x_5^2)x_1 - 2\varepsilon x_1(x_3 + x_5), \\ &\dot{x}_3 = x_4, \quad \dot{x}_4 = \nu x_3 - (x_1^2 + x_3^2 + 8x_5^2)x_3 - \varepsilon(x_1^2 + 2\delta x_3 x_5), \\ &\dot{x}_5 = x_6, \quad \dot{x}_6 = -\omega^2 x_5 - \alpha(x_1^2 + \beta x_3^2 + 2x_5^2)x_5 - \varepsilon(x_1^2 + \delta x_3^2), \end{aligned} \tag{5.1}$$

where α, β, δ, ν and ω are positive constants. System (5.1) is reversible with respect to the involution $R : (x_1, x_2, x_3, x_4, x_5, x_6) \mapsto (x_1, -x_2, x_3, -x_4, x_5, -x_6)$, such that

$$\mathrm{Fix}(R) = \{x_2 = x_4 = x_6 = 0\}, \quad \mathrm{Fix}(-R) = \{x_1 = x_3 = x_5 = 0\}.$$

Furthermore, the origin O is a saddle-centre with eigenvalues ± 1, $\pm\sqrt{\nu}$ and $\pm\omega i$. When $\varepsilon = 0$, the (x_1, x_2, x_3, x_4)-space is invariant under the flow of (5.1), and the restriction to the invariant space becomes

$$\begin{aligned} &\dot{x}_1 = x_2, \quad \dot{x}_2 = x_1 - (x_1^2 + x_3^2)x_1, \\ &\dot{x}_3 = x_4, \quad \dot{x}_4 = \nu x_3 - (x_1^2 + x_3^2)x_3. \end{aligned} \tag{5.2}$$

It was shown in [25] that there are four isolated homoclinic orbits if $\nu \neq 1$, and that there exists a one-parameter family of homoclinic orbits if $\nu = 1$. We therefore discuss the two cases $\nu \not\approx 1$ and $\nu \approx 1$ separately in the following.

5.1 The case $\nu \not\approx 1$

For $\varepsilon = 0$ four isolated homoclinic orbits of (5.1) are given by

$$x_\pm^h(t) = (\pm\sqrt{2}\,\mathrm{sech}\,t, \mp\sqrt{2}\,\mathrm{sech}\,t\,\tanh t, 0, 0, 0, 0) \tag{5.3}$$

and

$$\tilde{x}_\pm^h(t) = (0, 0, \pm\sqrt{2\nu}\,\mathrm{sech}\sqrt{\nu}\,t, \mp\sqrt{2\nu}\,\mathrm{sech}\sqrt{\nu}\,t\,\tanh\sqrt{\nu}\,t, 0, 0). \tag{5.4}$$

Let $z^s = (1, -1, 0, 0, 0, 0)$ and $\tilde{z}^s = (0, 0, 1, -\sqrt{\nu}, 0, 0)$. We find that $z_0 = (0, \mp 1, 0, 0, 0, 0)$, $Z^s = \mathrm{span}\{z_0, z^s\}$ and $\bar{Z} = \mathrm{span}\{z^s, e_3, e_5, e_6\}$ for $x_\pm^h(t)$, and $z_0 = (0, 0, 0, \mp 1, 0, 0)$, $Z^s = \mathrm{span}\{z_0, \tilde{z}^s\}$ and $\bar{Z} = \mathrm{span}\{\tilde{z}^s, e_1, e_5, e_6\}$ for $\tilde{x}_\pm^h(t)$, where $e_j \in \mathbb{R}^6$ denotes the unit vector of which only the j-th element is nonzero. The VE (3.2) becomes a triple of decoupled second-order ODEs. In particular, the fifth and sixth component of its homogeneous part is given by

$$\dot{\xi}_5 = \xi_6, \quad \dot{\xi}_6 = -(\omega^2 + 2\alpha\,\mathrm{sech}^2 t)\xi_5 \tag{5.5}$$

for $x_\pm^h(t)$, and

$$\dot{\xi}_5 = \xi_6, \quad \dot{\xi}_6 = -(\omega^2 + 2\alpha\beta\nu\,\mathrm{sech}^2\sqrt{\nu}\,t)\xi_5 \tag{5.6}$$

for $\tilde{x}^h_\pm(t)$.

As in Section 4, taking α as the control parameter, we have

$$\hat{\Xi}_6(\alpha) = 2\int_0^\infty \Psi_{55}(t;\alpha,\omega)\,\mathrm{sech}^2 t\,dt, \tag{5.7}$$

for $x^h_\pm(t)$, and

$$\begin{aligned}\hat{\Xi}_6(\alpha) =& 2\delta\int_0^\infty \Psi_{55}(\sqrt{\nu}\,t;\alpha\beta,\omega/\sqrt{\nu})\,\mathrm{sech}^2\sqrt{\nu}\,t\,dt\\ =& 2\delta\int_0^\infty \Psi_{55}(t;\alpha\beta,\omega/\sqrt{\nu})\,\mathrm{sech}^2 t\,dt\end{aligned} \tag{5.8}$$

for $\tilde{x}^h_\pm(t)$, where $\Psi_{55}(t;\alpha,\omega)$ is the ξ_5-component of the solution of (5.5) with initial conditions $(\xi_5(0),\xi_6(0)) = (1,0)$. Note that $\Psi_{55}(\sqrt{\nu}\,t;\alpha\beta,\omega/\sqrt{\nu})$ is the ξ_5-component of the solution of (5.5) with $(\xi_5(0),\xi_6(0)) = (1,0)$. For both $x^h_\pm(t)$ and $\tilde{x}^h_\pm(t)$, we can find an element $z \in \tilde{\mathscr{C}}$ such that $z_2 = z_4 = 0$ and $z_6 = \hat{\Xi}_6(\alpha)$, where $\tilde{\mathscr{C}}$ was defined by (3.11). Thus, if $\hat{\Xi}_6$ in (5.7) or (5.8) has a simple zero at $\alpha = \alpha_0$, then the condition of Theorem 3.3 holds for the value of α.

From the analysis of Section 4, we easily see that $\hat{\Xi}_6$ in (5.7) or (5.8) has a simple zero at

$$\alpha \quad \text{or} \quad \alpha\beta = 3, 10, 21, 36, 55, 78, \ldots. \tag{5.9}$$

Applying Theorem 3.3, we see that for $\alpha = 3, 10, 21, \ldots$ a new branch of homoclinic orbits bifurcates from $x^h_\pm(t)$. Similarly, a new branch of homoclinic orbits bifurcates from $\tilde{x}^h_\pm(t)$ if $\alpha\beta = 3, 10, 21, \ldots$. These results are illustrated in Figs. 6 and 7, where as before we used `AUTO/HomCont` for the numerical computations.

5.2 The case $\nu \approx 1$

Let $\nu = 1 + \varepsilon\bar{\nu}$ in (5.1), where $\bar{\nu} = \mathscr{O}(1)$ is some constant. A one-parameter family of homoclinic orbits for $\varepsilon = 0$ is given by

$$\begin{aligned}x^h(t;\theta) =& (\sqrt{2}\cos\theta\,\mathrm{sech}\,t, -\sqrt{2}\cos\theta\,\mathrm{sech}\,t\,\tanh t,\\ & \sqrt{2}\sin\theta\,\mathrm{sech}\,t, -\sqrt{2}\sin\theta\,\mathrm{sech}\,t\,\tanh t, 0, 0),\end{aligned} \tag{5.10}$$

with the parameter $\theta \in [-\pi,\pi)$. Observe that the homoclinic orbits with $\theta = 0$ and $\theta = -\pi$, respectively, correspond to $x^h_+(t)$ and $x^h_-(t)$ in the case of $\nu \not\approx 1$, while the homoclinic orbits with $\theta = \pm\pi/2$ correspond to $\tilde{x}^h_\pm(t)$. Let $z^s(\theta) = (-\sin\theta, 0, -\cos\theta, 0, 0, 0)$. Then $T_{x^h(0;\theta)}\mathscr{M}_0 = \mathrm{span}\{z^s(\theta)\}$. We also have $z_0(\theta) = (0, -\cos\theta, 0, -\sin\theta, 0, 0)$, $Z^s(\theta) = \mathrm{span}\{z_0(\theta), z^s(\theta)\}$ and

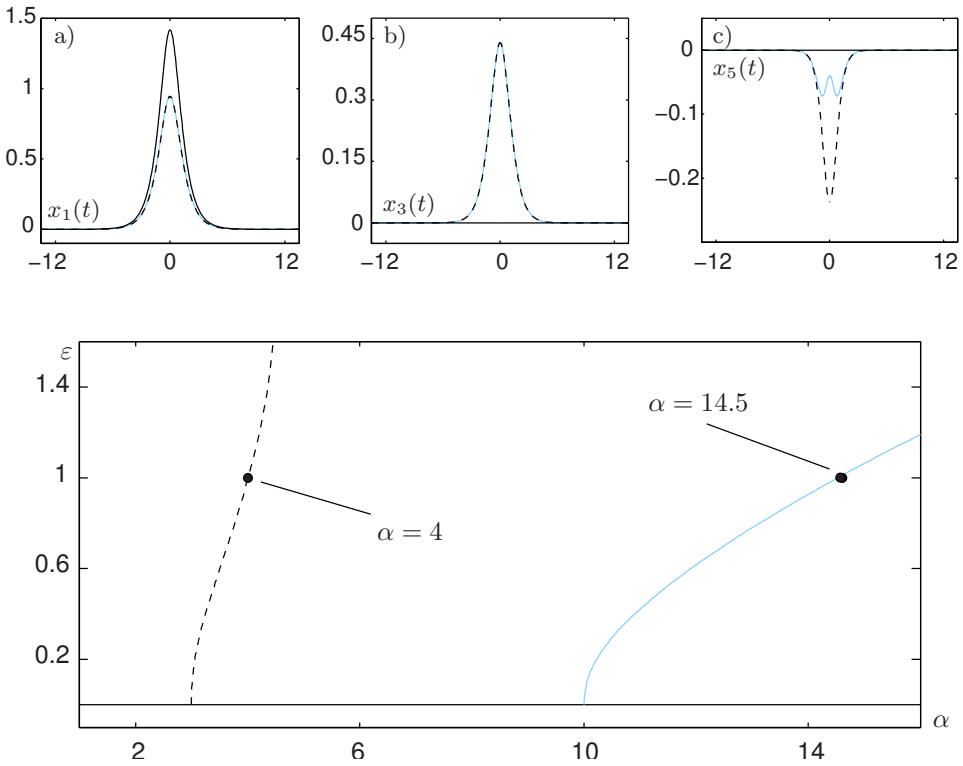

Fig. 6. Numerically computed branches of symmetric homoclinic orbits bifurcating from $x^h_+(t)$ in (5.1) for $\nu = \beta = 2$ and $\omega = 1$. Panels a)–c) contain plots of the x_1, x_3 and x_5 components of the primary solution (black, solid) and of the bifurcating solutions (in the same line style as the bifurcation curves in the main panel) at $\varepsilon = 1$.

$\bar{Z}(\theta) = \mathrm{span}\{\bar{z}^s(\theta), \bar{z}_0(\theta), e_5, e_6\}$, where

$$\bar{z}^s(\theta) = (\cos\theta, 0, -\sin\theta, 0, 0, 0), \quad \bar{z}_0(\theta) = (0, \sin\theta, 0, -\cos\theta, 0, 0).$$

The VE (3.2) is given by

$$\begin{aligned}
\dot{\xi}_1 &= \xi_2, \quad \dot{\xi}_2 = (1 - 2(2 + \cos 2\theta)\,\mathrm{sech}^2 t)\xi_1 - (2\sin 2\theta\,\mathrm{sech}^2 t)\xi_3 \\
&\qquad - 2\sin 2\theta\,\mathrm{sech}^2 t, \\
\dot{\xi}_3 &= \xi_4, \quad \dot{\xi}_4 = -(2\sin 2\theta\,\mathrm{sech}^2 t)\xi_1 + (1 - 2(2 - \cos 2\theta)\,\mathrm{sech}^2 t)\xi_3 \\
&\qquad + \sqrt{2}\,\bar{\nu}\sin\theta\,\mathrm{sech}\ t - 2\cos^2\theta\,\mathrm{sech}^2 t, \\
\dot{\xi}_5 &= \xi_6, \quad \dot{\xi}_6 = -(\omega^2 + 2\alpha(\cos^2\theta + \beta\sin^2\theta)\,\mathrm{sech}^2 t)\xi_5 \\
&\qquad - 2(\cos^2\theta + \delta\sin^2\theta)\mathrm{sech}^2 t.
\end{aligned} \tag{5.11}$$

By the change of coordinates

$$\begin{pmatrix} \bar{\xi}_j \\ \bar{\xi}_{j+2} \end{pmatrix} = \begin{pmatrix} \cos\theta & \sin\theta \\ -\sin\theta & \cos\theta \end{pmatrix} \begin{pmatrix} \xi_j \\ \xi_{j+2} \end{pmatrix}, \quad j = 1, 2, \tag{5.12}$$

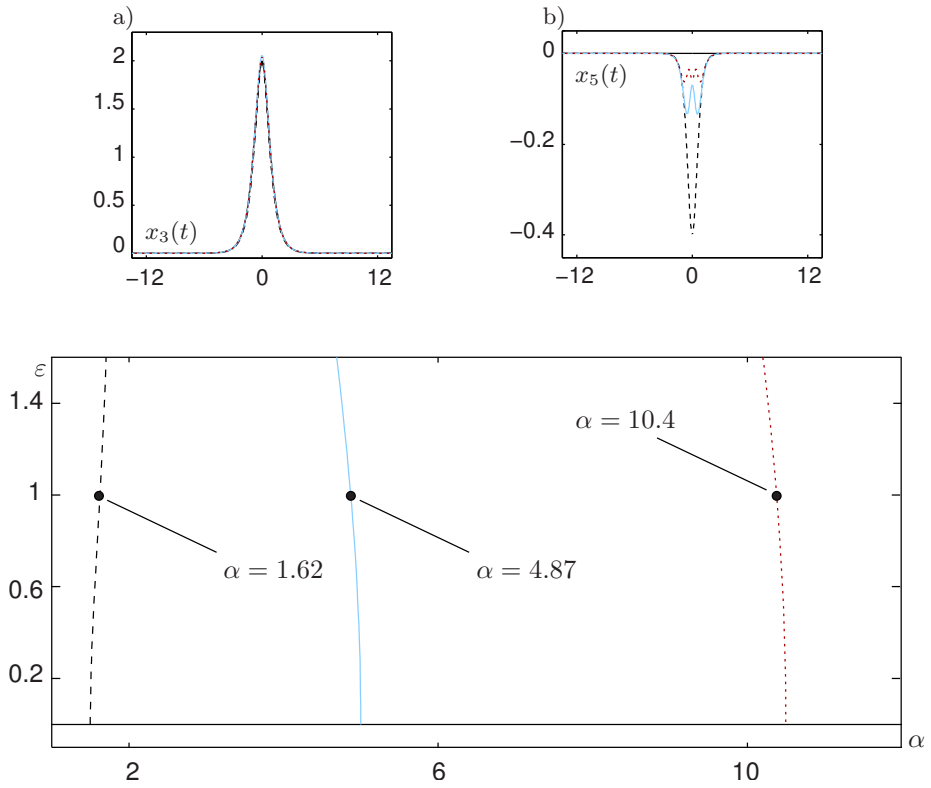

Fig. 7. Numerically computed branches of symmetric homoclinic orbits bifurcating from $\tilde{x}^h_+(t)$ in (5.1) for $\nu = \beta = 2$ and $\omega = 1$. Panels a) and b) contain plots of the x_3, and x_5 components of the bifurcating solutions (in the same line style as the bifurcation curves in the main panel) at $\varepsilon = 1$. Note that the x_1 component is not shown, since it is zero for all solutions.

the first four equations of (5.11) are transformed to

$$\begin{aligned}
\dot{\bar{\xi}}_1 = \bar{\xi}_2, \quad \dot{\bar{\xi}}_2 =&(1 - 6\,\mathrm{sech}^2 t)\bar{\xi}_1 - \frac{3}{2}(\sin\theta + \sin 3\theta)\,\mathrm{sech}^2 t \\
&+ \sqrt{2}\,\bar{\nu}\,\sin^2\theta\,\mathrm{sech}\,t, \\
\dot{\bar{\xi}}_3 = \bar{\xi}_4, \quad \dot{\bar{\xi}}_4 =&(1 - 2\,\mathrm{sech}^2 t)\bar{\xi}_3 - \frac{1}{2}(\cos\theta + 3\cos 3\theta)\,\mathrm{sech}^2 t \\
&+ \sqrt{2}\,\bar{\nu}\,\sin\theta\cos\theta\,\mathrm{sech}\,t.
\end{aligned} \tag{5.13}$$

Taking α as the control parameter we find in the new coordinates

$$\begin{aligned}
\hat{\Xi}_4(\theta) =&\frac{1}{2}(\cos\theta + 3\cos 3\theta)\int_0^\infty \Psi_{33}(t)\,\mathrm{sech}^2 t\,dt \\
&- \sqrt{2}\,\bar{\nu}\,\sin\theta\cos\theta\int_0^\infty \Psi_{33}(t)\,\mathrm{sech}\,t\,dt, \\
\hat{\Xi}_6(\alpha,\theta) =&2(\cos^2\theta + \delta\sin^2\theta)\int_0^\infty \Psi_{55}(t;\alpha,\theta)\,\mathrm{sech}^2 t\,dt,
\end{aligned} \tag{5.14}$$

where $\Psi_{33}(t)$ (resp. $\Psi_{55}(t;\alpha)$) is the $\bar{\xi}_3$-component (resp. $\bar{\xi}_5$-component) of the

solution to the homogeneous part of (5.13) (resp. (5.11)) with $(\bar{\xi}_3(0), \bar{\xi}_4(0)) = (1, 0)$ (resp. $(\xi_5(0), \xi_6(0)) = (1, 0)$). Moreover, in the new coordinates, $z_0(\theta) \mapsto -e_2$ and $z^s(\theta) \mapsto (-\sin 2\theta, 0, -\cos 2\theta, 0, 0, 0)$, while the expression of $\mathrm{Fix}(R)$ is unchanged. Hence, we find an element $z \in \tilde{\mathscr{C}}$ such that $z_2 = 0$, $z_4 = \hat{\Xi}_4(\theta)$ and $z_6 = \hat{\Xi}_6(\alpha, \theta)$ in the new coordinates. Thus, if $(\hat{\Xi}_4(\theta), \hat{\Xi}_6(\alpha, \theta))$ has a simple zero at $(\alpha, \theta) = (\alpha_0, \theta_0)$, then the condition of Theorem 3.3 is fulfills for these parameter values. Consequently, we find a family of homoclinic orbits bifurcating off the primary branch at $\alpha = \alpha_0$.

We have

$$\Psi_{33}(t) = \operatorname{sech} t$$

and compute

$$\hat{\Xi}_4(\theta) = \frac{\pi}{8}(\cos\theta + 3\cos 3\theta) - \sqrt{2}\,\bar{\nu}\,\sin\theta\cos\theta.$$

Hence, $\hat{\Xi}_4(\theta)$ has a simple zero at

$$\theta = \pm\frac{\pi}{2} \tag{5.15}$$

and

$$\theta = -\theta_\pm, \quad \theta = \mp\pi + \theta_\pm, \tag{5.16}$$

where

$$\theta_\pm = \arcsin\left(\frac{\sqrt{2}\,\bar{\nu} \pm \sqrt{3\pi^2 + 2\,\bar{\nu}^2}}{3\pi}\right) \in [-\pi/2, \pi/2].$$

On the other hand, from the analysis of Section 4 we easily see that for the values of θ in (5.15) or (5.16) $\hat{\Xi}_6(\alpha, \theta)$ has a simple zero at

$$\alpha\beta \quad \text{or} \quad \alpha(\cos^2\theta_\pm + \beta\sin^2\theta_\pm) = 3, 10, 21, 36, 55, 78, \ldots. \tag{5.17}$$

Applying Theorem 3.3, we see that for $\varepsilon > 0$ sufficiently small, the system (5.1) has a symmetric homoclinic orbit to O near $x^h(t;\theta)$ at the values of α and θ approximately given by (5.15)-(5.17) for each value of $\bar{\nu}$. This orbit bifurcates from the primary one, $x^h(t;\theta)$ with θ given by (5.15) or (5.16), at the points of (5.17) on the ε-axis. Moreover, the three branches $\theta = -\pi/2$, $-\theta_+$ and $-\pi + \theta_+$ (resp. $\theta = \pi/2$, $-\theta_-$ and $\pi + \theta_-$) meet near

$$(\bar{\nu}, \theta) = \left(\frac{\pi}{\sqrt{2}}, -\frac{\pi}{2}\right) \quad \left(\text{resp. } \left(-\frac{\pi}{\sqrt{2}}, \frac{\pi}{2}\right)\right).$$

In the $(\bar{\nu}, \alpha)$-parameter plane, the branching points exist at $\bar{\nu} = \pm\pi/\sqrt{2}$ and

$$\alpha\beta = 3, 10, 21, 36, 55, 78, \ldots.$$

These results are summarised in Fig. 8. In the two top panels in this figure the bifurcation diagrams for symmetric homoclinic orbits in the $(\bar{\nu}, \theta)$ parameter

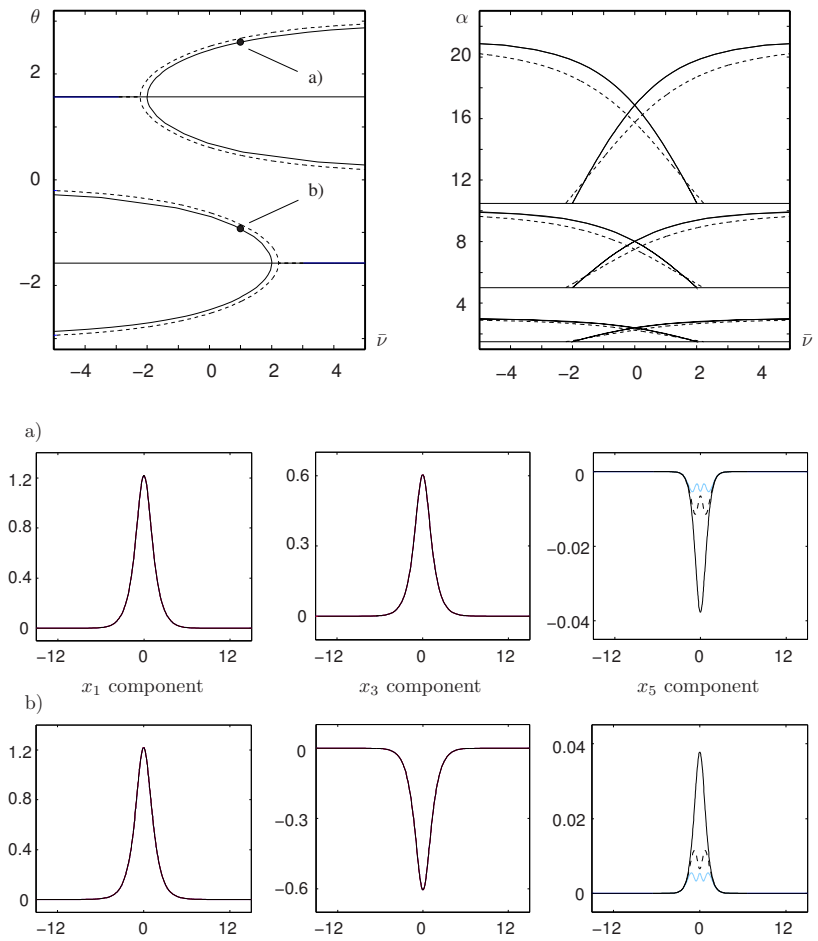

Fig. 8. Bifurcation diagrams and plots of solutions for (5.1) for $\varepsilon = 0.1$, $\beta = 2$ and $\omega = 1$. The bifurcation diagrams contain both the theoretical predictions (dashed) and numerical computations (solid). In parts a) and b) plots of the x_1, x_3 and x_5 components of the bifurcating solutions at the indicated points a), b) with $\bar{\nu} = 1$ in the $(\bar{\nu}, \theta)$ diagram are shown. The panels contain plots of the three solutions bifurcating at $\alpha = 1.5$ (black, solid), $\alpha = 5$ (black, dashed) and $\alpha = 10.5$ (grey, solid). The x_1- and x_3-components of these solutions are very similar.

plane and in the $(\bar{\nu}, \alpha)$ parameter plane are shown for $\beta = 2$ and $\omega = 1$. Both the theoretical predictions (dashed) and the numerical computations (solid curves) are shown in the diagrams. Again, the continuation software `AUTO/HomCont` has been used to derive the numerical results. Here θ has been determined as

$$\theta = \arctan\left(\frac{x^h_{\varepsilon,3}(0)}{x^h_{\varepsilon,1}(0)}\right)$$

for the numerically computed, symmetric homoclinic orbit $x^h_\varepsilon(t)$, where $t = 0$ is the time at which $x^h_\varepsilon(t)$ intersects Fix(R).

The scenario depicted in Fig. 8 reveals a symmetry-breaking bifurcation of

homoclinic orbits. Indeed, observe that (5.1) is $\mathbb{Z}_2$-symmetric with respect to

$$S : (x_1, x_2, x_3, x_4, x_5, x_6) \mapsto (-x_1, -x_2, x_3, x_4, x_5, x_6),$$

such that in particular the space $\mathrm{Fix}(S) = \{x_1 = x_2 = 0\}$ is invariant under the flow of the system. The homoclinic solutions $\tilde{x}^h_\pm$, which correspond to the solutions with $\theta = \pm\pi/2$ in (5.10), are contained in $\mathrm{Fix}(S)$ and undergo a symmetry-breaking bifurcation (at different values of $\bar{\nu}$), thereby giving rise to new branches of homoclinic solutions. This symmetry-breaking bifurcation is illustrated in the left top panel of Fig. 8.

In the panels below the bifurcation diagrams we give an impression of the bifurcating solutions by plotting their x_1, x_3 and x_5 components. Note that we restrict to showing one bifurcating solution from each of the new branches in the $(\bar{\nu}, \theta)$ bifurcation diagram, since the solution on the other arc of this branch is the symmetric counterpart.

6 Conclusions

In this paper we have developed a perturbation technique for detecting the existence of symmetric homoclinic orbits to saddle-centres in reversible systems of ODEs. For this we have extended the well-known Melnikov method to derive an approximation to the corresponding stable and unstable manifolds. We have applied the method to the analysis of homoclinic orbits to saddle-centres in two examples. Besides the mere existence results we have demonstrated how the method can be used to obtain information about bifurcations of homoclinic orbits in specific systems. Numerical studies have shown good agreement with the theoretical predictions.

Our technique is of importance in applications since homoclinic orbits to saddle-centre equilibria often appear as embedded solitons (ESs) in systems of PDEs, as stated in the Introduction. One of the fascinating features of ESs is their semi-stability, which has been established explicitly in a number of examples [28, 29]. These solutions are linearly stable, but are subject to a weak nonlinear one-sided instability [4, 29]. This means that if one makes an energy increasing perturbation then via the shedding of radiation, the initial condition relaxes algebraically back to the solitary wave. In contrast, an energy decreasing perturbation would cause the solitary wave to decay algebraically away. It is a challenging problem to decide whether the homoclinic orbits detected by our method give rise to semi-stable ESs in corresponding PDEs. In particular, when the primary ESs with $\varepsilon = 0$ are stable or semi-stable it is very interesting to determine the semi-stability of ESs bifurcating from them. These problems, however, cannot be solved within the finite-dimensional framework

of dynamical systems theory employed here.

Let us finally comment on some dynamical consequences of the investigations in this paper. A number of studies has dealt with the existence of multi-pulse homoclinic orbits near a primary homoclinic orbit to a saddle-centre equilibrium. For reversible (analytic) Hamiltonian systems having a homoclinic orbit to a saddle centre it has been shown in [10, 15] that infinitely many multi-pulse homoclinic orbits in any neighbourhood of the original system exist, if the so-called Birkhoff signature condition and an additional transversality condition are satisfied. Specifically, the transversality condition requires that the linearised dynamics along the homoclinic orbit is not purely rotational in conjugate canonical coordinates. The existence of such coordinates near saddle-centres is guaranteed by the results in [18, 19]. If both conditions are fulfilled then in a generic unfolding there exists an infinite sequence of parameter values, accumulating from both sides at the critical value for the primary homoclinic orbit, at which the unfolded system possesses a two-pulse homoclinic orbit to O. In contrast, studies in [2] suggest that in purely reversible systems this accumulation occurs only on one side of the primary homoclinic solution, independent of the Birkhoff signature.

In the context of our studies it would be interesting to analyse the accumulation of multi-pulse homoclinic orbits near one of the branching points of the primary homoclinic orbits. For this note that the above mentioned transversality condition also implies that a horseshoe is created and chaotic dynamics occurs in the unperturbed system [9, 12, 15, 26]. Moreover, if the unperturbed system has an invariant plane on which a homoclinic orbit exists, then the normal variational equation (NVE), which consists of components normal to the invariant plane of the VE, for the homoclinic orbit, is not integrable in the meaning of the differential Galois theory [16, 17]. In particular, in the example (4.1) from Section 4, the NVE is given by (4.7) and both conditions are equivalent [27]. Thus, for the Hamiltonian case, if the system (4.1) exhibits chaotic dynamics and has an infinity of multi-pulse homoclinic orbits in any neighbourhood of $\varepsilon = 0$, then the homoclinic orbits (4.5) cannot be continued for $\varepsilon > 0$. Taking into account recent general results for reversible systems [2, 7], we expect the same consequence for non-Hamiltonian reversible systems.

Acknowledgements

The authors thank Alan Champneys and Boris Malomed for useful discussions and helpful suggestions. K.Y. acknowledges support from the Japan Society for the Promotion of Science (JSPS), which enabled him to stay in Bristol and to perform this work. T.W.'s research has been supported by the EPSRC grant number GR/535684/01.

A Solutions of equation (4.7)

In this appendix we give necessary information on solutions of (4.7) or equivalently the second-order differential equation,

$$\ddot{\eta} + (\omega^2 + 2\alpha \operatorname{sech}^2 t)\eta = 0. \tag{A.1}$$

A.1 The general non-integrable case

We first use the transformations

$$z = \frac{1}{2}(1 - \tanh t), \quad \zeta = (4z(1-z))^{-i\omega/2}\eta \tag{A.2}$$

to transform (A.1) into

$$z(1-z)\frac{d^2\zeta}{dz^2} + (1+i\omega)(1-2z)\frac{d\zeta}{dz} - (i\omega - \rho)(i\omega + \rho + 1)\zeta = 0, \tag{A.3}$$

which is the Gauss hypergeometric equation (4.10) with $c_1 = i\omega - \rho$, $c_2 = i\omega + \rho + 1$ and $c_3 = 1 + i\omega$, where ρ is given by (4.13). A special solution to (A.3) is given by

$$\zeta(t) = \left(\frac{z}{2}\right)^{-i\omega} F(-\rho, \rho + 1, 1 - i\omega; z)$$

(see Eq. (4.11)), which yields a complex solution of (A.1)

$$\hat{\eta}(t) = e^{i\omega t} F(-\rho, \rho + 1, 1 - i\omega; (1 - \tanh t)/2) \tag{A.4}$$

by the inverse of (A.2). When t is real, the general solution of (A.1) is given by

$$\eta(t) = C_1(F_R(t)\cos\omega t - F_I(t)\sin\omega t) + C_2(F_R(t)\sin\omega t + F_I(t)\cos\omega t), \tag{A.5}$$

where C_1 and C_2 are arbitrary constants, since the real and imaginary parts of (A.4) also represent two independent solutions of (A.1).

Obviously,

$$\hat{\eta}(t) \to e^{i\omega t} \quad \text{as } t \to \infty \tag{A.6}$$

since $F(-\rho, \rho+1, 1-i\omega; 0) = 1$. In addition, since by Formula 15.3.6 of [1]

$$\begin{aligned} &F(-\rho, \rho+1, 1-i\omega; z) \\ &= \frac{\Gamma(1-i\omega)\Gamma(-i\omega)}{\Gamma(1+\rho-i\omega)\Gamma(-\rho-i\omega)} F(-\rho, \rho+1, 1+i\omega; 1-z) \\ &\quad + \frac{\Gamma(1-i\omega)\Gamma(i\omega)}{\Gamma(-\rho)\Gamma(\rho+1)} (1-z)^{-i\omega} F(1-i\omega+\rho, -i\omega-\rho, 1-i\omega; 1-z) \end{aligned}$$

and by Formulas 6.1.15, 6.1.28 and 6.1.29 of [1]

$$\frac{\Gamma(1-i\omega)\Gamma(i\omega)}{\Gamma(-\rho)\Gamma(\rho+1)} = i\frac{\sin \pi\rho}{\sinh \pi\omega},$$

we have

$$\hat{\eta}(t) \to (a_R + ia_I)e^{i\omega t} + ib_I e^{-i\omega t} \quad \text{as } t \to -\infty, \tag{A.7}$$

where a_R, a_I and b_I are given in (4.14). Moreover, by Formula 15.1.26 of [1]

$$\hat{\eta}(0) = \frac{2^{i\omega}\sqrt{\pi}\,\Gamma(1-i\omega)}{\Gamma(1/2-\rho/2-i\omega/2)\Gamma(1+\rho/2-i\omega/2)} = c_R + ic_I. \tag{A.8}$$

We determine C_1 and C_2 for (A.5) to satisfy $(\eta(0), \dot{\eta}(0)) = (1, 0)$. From (A.6) and (A.7) we see that

$$\eta(t) \to C_1 \cos \omega t + C_2 \sin \omega t \quad \text{as } t \to \infty$$

and

$$\eta(t) \to C_1[a_R \cos \omega t + (-a_I + b_I) \sin \omega t] + C_2[(a_I + b_I) \cos \omega t + a_R \sin \omega t]$$

as $t \to -\infty$. Since $\eta(t)$ also has to be symmetric, i.e., $\eta(t) = \eta(-t)$, we have

$$C_1 = C_1 a_R + C_2(a_I + b_I), \quad C_2 = -C_1(-a_I + b_I) - C_2 a_R, \tag{A.9}$$

which has multiple nonzero roots as a system of equations for C_1 and C_2 since $a_R^2 + a_I^2 - b_I^2 = 1$ (see Eq. (5.7) of [26]). Moreover, since $\eta(0) = 1$,

$$C_1 c_R + C_2 c_I = 1 \tag{A.10}$$

by (A.8). We solve (A.9) and (A.10) for C_1 and C_2 to obtain

$$C_1 = \frac{a_I + b_I}{(a_I + b_I)c_R + (1 - a_R)c_I}, \quad C_2 = \frac{1 - a_R}{(a_I + b_I)c_R + (1 - a_R)c_I}$$

unless the denominator is zero. Thus, we see that Eq. (4.12) gives the $(3,3)$-component of the fundamental matrix, $\Psi_{33}(t; \alpha)$, if $(a_I + b_I)c_R + (1 - a_R)c_I \neq 0$.

A.2 The integrable case

Now we restrict ourself to the integrable case of $\alpha = l(l-1)/2$, i.e., $\rho = l-1$, with $l \in \mathbb{N}$. In this case the hypergeometric series (4.9) with $c_1 = -\rho$, $c_2 = \rho+1$ and $c_3 = 1 - i\omega$ terminates at $k = \rho = l-1$. Moreover, $b_I = 0$,

$$a_R + i a_I = \begin{cases} 1 & \text{if } l = 1; \\ \dfrac{(1-l-i\omega)\cdots(-1-i\omega)}{(l-1-i\omega)\cdots(1-i\omega)} & \text{if } l \geq 2, \end{cases} \tag{A.11}$$

and

$$c_R + i c_I = \begin{cases} 1 & \text{if } l = 1; \\ \dfrac{(1-m-i\omega/2)\cdots(-i\omega/2)}{(m-1/2-i\omega/2)\cdots(1/2-i\omega/2)} & \text{if } l = 2m; \\ \dfrac{(-m+1/2-i\omega/2)\cdots(-1/2-i\omega/2)}{(m-i\omega/2)\cdots(1-i\omega/2)} & \text{if } l = 2m+1, \end{cases} \tag{A.12}$$

where $m \in \mathbb{N}$, since $\Gamma(z+1) = z\Gamma(z)$ and

$$\frac{2^{i\omega}\sqrt{\pi}\,\Gamma(1-i\omega)}{\Gamma(1/2-i\omega/2)\Gamma(1-i\omega/2)} = 1$$

by Formula 6.1.18 of [1]. Using (4.9), (4.12), (A.11) and (A.12), we can compute $\Psi_{33}(t;\alpha)$. This is demonstrated explicitly for the cases $l = 1, 2, 3$ below.

A.2.1 Case of $l = 1$

From (4.9), (A.11) and (A.12) we obtain $F(0, 1, 1-i\omega; (1-\tanh t)/2) = 1$, $a_R = c_R = 1$ and $a_I = c_I = 0$. Obviously, $(a_I + b_I)c_R + (1 - a_R)c_I = 0$ and hence Eq. (4.12) is not valid. However, in this case, we can also solve (A.9) and (A.10) directly to obtain $C_1 = 1$ and $C_2 = 0$, so that

$$\Psi_{33}(t;0) = \cos\omega t.$$

A.2.2 Case of $l = 2$

From (4.9), (A.11) and (A.12),

$$\begin{aligned} &F(-1, 2, 1-i\omega; (1-\tanh t)/2) \\ &= 1 - \frac{2}{1-i\omega}(1-\tanh t) = \frac{1}{1+\omega^2}[(\omega^2 + \tanh t) + i\omega(-1+\tanh t)] \end{aligned}$$

and

$$a_R = -\frac{1-\omega^2}{1+\omega^2}, \quad a_I = -\frac{2\omega}{1+\omega^2}, \quad c_R = \frac{\omega^2}{1+\omega^2}, \quad c_I = -\frac{\omega}{1+\omega^2}.$$

Hence, $C_1 = 1$ and $C_2 = -1/\omega$, so that

$$\Psi_{33}(t;1) = \cos\omega t - \frac{1}{\omega}\sin\omega t \tanh t.$$

A.2.3 Case of $l = 3$

From (4.9), (A.11) and (A.12),

$$\begin{aligned}
&F(-2,3,1-i\omega;(1-\tanh t)/2) \\
&= 1 - \frac{6}{1-i\omega}(1-\tanh t) + \frac{6}{(1-i\omega)(2-i\omega)}(1-\tanh t)^2 \\
&= \frac{1}{4+5\omega^2+\omega^4}\{[-(2+\omega^2-\omega^4) + 9\omega^2\tanh t + 3(2-\omega^2)\tanh^2 t] \\
&\quad + 3i\omega[-(1+\omega^2) - (2-\omega^2)\tanh t + 3\tanh^2 t)]\}
\end{aligned}$$

and

$$\begin{aligned}
a_R &= \frac{4-13\omega^2+\omega^4}{(1+\omega^2)(4+\omega^2)}, \quad a_I = \frac{6\omega(2-\omega^2)}{(1+\omega^2)(4+\omega^2)}, \\
c_R &= -\frac{2-\omega^2}{4+\omega^2}, \quad c_I = -\frac{3\omega^2}{4+\omega^2}.
\end{aligned}$$

Hence,

$$C_1 = -\frac{2-\omega^2}{1+\omega^2}, \quad C_2 = -\frac{3\omega^2}{1+\omega^2},$$

so that

$$\Psi_{33}(t;3) = \cos\omega t - \frac{3}{1+\omega^2}(\omega\sin\omega t\tanh t + \cos\omega t\tanh^2 t).$$

References

[1] M. Abramowitz and I.A. Stegun (eds.), *Handbook of Mathematical Functions with Formulas, Graphs, and Mathematical Tables*, Dover, New York, 1965.

[2] A.R. Champneys and J. Härterich, Cascades of homoclinic orbits to a saddle-centre for reversible and perturbed Hamiltonian systems, *Dyn. Stab. Sys.*, **15** (2000), 231–252.

[3] A.R. Champneys and B.A. Malomed, Embedded solitons in a three-wave system, *Phys. Rev. E*, **61** (1999), 463466.

[4] A. R. Champneys, B. A. Malomed, J. Yang, and D. J. Kaup. Embedded solitons: solitary waves in resonance with the linear spectrum. *Physica D*, **152** (2001), 340–354.

[5] E.A. Coddington and N. Levinson, *Theory of Ordinary Differential Equations*, McGraw-Hill, New York, 1955.

[6] E. Doedel, A.R. Champneys, T.F. Fairgrieve, Y.A. Kuznetsov, B. Sandstede and X. Wang, *AUTO97: Continuation and Bifurcation Software for Ordinary Differential Equations (with HomCont)*, Concordia University, Montreal, 1997.

[7] A. Delshams and J.T. Lázaro, Pseudo-normal form near saddle-center or saddle-focus equilibria, *J. Diff. Eqn.*, **208**(2) (2005), 312–343.

[8] A. Erdélyi, *Higher Transcendental Functions*, Vol. I, McGraw-Hill, New York, 1953.

[9] C. Grotta-Ragazzo, Nonintegrability of some Hamiltonian systems, scattering and analytic continuation, *Commun. Math. Phys.*, **166** (1994), 255–277.

[10] C. Grotta-Ragazzo, Irregular dynamics and homoclinic orbits to Hamiltonian saddle centers, *Commun. Pure Appl. Math.*, **50** (1997), 105–147.

[11] J. Guckenheimer and P.J. Holmes, *Nonlinear Oscillations, Dynamical Systems, and Bifurcations of Vector Fields*, Springer, New York, 1983.

[12] L.M. Lerman, Hamiltonian systems with loops of a separatrix of a saddle-center, *Selecta Math. Sov.*, **10** (1991), 297–306.

[13] B.A. Malomed, T. Wagenknecht, A.R. Champneys and M.J. Pearce, Accumulation of embedded solitons in systems with quadratic nonlinearity, *Chaos*, to appear (2005).

[14] K.R. Meyer and G.R. Hall, *Introduction to Hamiltonian Dynamical Systems and the N-Body Problem*, Springer, New York, 1992.

[15] A. Mielke, P.J. Holmes and O. O'Reilly, Cascades of homoclinic orbits to, and chaos near, a Hamiltonian saddle-center, *J. Dyn. Diff. Eqn.*, **4** (1992), 95–126.

[16] J.J. Morales-Ruiz, *Differential Galois Theory and Non-Integrability of Hamiltonian systems*, Birkhäuser, Basel, 1999.

[17] J.J. Morales-Ruiz and J.M. Peris, On a Galoisian approach to the splitting of separatrices, *Ann. Fac. Sci. Toulouse Math.*, **8** (1999), 125–141.

[18] J. Moser, On the generalization of a theorem of A. Liapunoff, *Commun. Pure Appl. Math.*, **11** (1958), 257–271.

[19] H. Rüssmann, Über das Verhalten analytischer Hamiltonscher Differentialgleichungen in der Nähe einer Gleichgewichtslösung, *Math. Ann.*, **154**, (1964), 285–300.

[20] I. Towers, A.V. Buryak, R.A. Sammut and B.A. Malomed, Stable localized vortex solitons, *Phys. Rev. E*, **63** (2001), 055601.

[21] A. Vanderbauwhede and B. Fiedler. Homoclinic period blow-up in reversible and conservative systems. *Z. Angew. Math. Phys.*, **43** (1992), 292–318.

[22] M. Van der Put and M.F. Singer, *Galois Theory of Linear Differential Equations*, Springer, New York, 2003.

[23] S. Wiggins, *Introduction to Applied Nonlinear Dynamical Systems and Chaos*, Springer, New York, 1990.

[24] S. Wolfram, *The Mathematica Book*, 5th ed. (Wolfram Media, Champaign, IL, 2003).

[25] K. Yagasaki, The method of Melnikov for perturbations of multi-degree-of-freedom Hamiltonian systems, *Nonlinearity*, **12** (1999), 799–822.

[26] K. Yagasaki, Horseshoes in two-degree-of-freedom Hamiltonian systems with saddle-centers, *Arch. Rational Mech. Anal.*, **154** (2000), 275–296.

[27] K. Yagasaki, Galoisian obstructions to integrability and Melnikov criteria for chaos in two-degree-of-freedom Hamiltonian systems with saddle-centers, *Nonlinearity*, **16** (2003), 2003–2012.

[28] J. Yang, Dynamics of embedded solitons in the extended KdV equations, *Stud. Appl. Math.* **106** (2001), 337-365.

[29] J. Yang, B.A. Malomed, D.J. Kaup and A.R. Champneys, Embedded solitons: A new type of solitary wave, *Math. Comp. Sim.*, **56** (2001), 585–600.